

Synthesis and Catalytic Abilities of Silica-coated Fe₃O₄ Nanoparticle Bonded Metalloporphyrins with Different Saturation Magnetization

Chang-Xiang Liu · Qiang Liu · Can-Cheng Guo

Received: 3 April 2010/Accepted: 18 May 2010/Published online: 2 June 2010
© Springer Science+Business Media, LLC 2010

Abstract In this paper, a series of nanoparticle bonded metalloporphyrins with different saturation magnetization were synthesized by a modified silanation method. Under geomagnetic field (5×10^{-5} T), with the increase of the saturation magnetizations, the growth rate of yields of cyclohexanol in the cyclohexane oxidation with iodosylbenzene catalyzed by these nanoparticle bonded metalloporphyrins followed the order of ironporphyrin > manganeseporphyrin > cobaltporphyrin.

Keywords Nanoparticle · Metalloporphyrin · Cyclohexane oxidation · Saturation magnetization · Catalysis

1 Introduction

Since the discovery of magnetic Fe₃O₄ nanoparticles in many organisms [1], the influence of magnetic field on chemical reactions has received extensive attention. Researchers have confirmed that, through the transduction of free radicals, a weak magnetic field on chemical reactions often produces magnetic amplification [2]. Metalloporphyrins, as the biomimetic catalysts models of cytochrome P-450 mono-oxygenase, have been widely used in the aerobic oxidations of alkanes under mild conditions [3–5]. Guo et al. have studied the cyclohexane oxidation with iodosylbenzene (PhIO) catalyzed by metalloporphyrins under the external magnetic field, and the experimental results showed that the influence of magnetic field on the catalytic abilities

of different metalloporphyrins was different, and the influence on the catalytic ability of ironporphyrin was much greater than the ones of other metalloporphyrins. These results indicated that it is natural choice for cytochrome P-450 mono-oxygenase with ironporphyrin structure [6]. Ji et al. [7, 8] have attempted to immobilize metalloporphyrins on magnetic Fe₃O₄ nanoparticles by copolymerizing styrene with metalloporphyrins in the presence of Fe₃O₄ magnetic fluid, and the obtained magnetic polymer microspheres immobilizing metalloporphyrins in the cyclohexane oxidation with molecular oxygen could be easily separated and recovered with the aid of a magnet. Nevertheless, under geomagnetic field (5×10^{-5} T), the influence of the saturation magnetizations of magnetic Fe₃O₄ nanoparticles on the catalytic abilities of metalloporphyrins remains to be highly desirable.

In this study, a series of silica-coated Fe₃O₄ nanoparticles with different saturation magnetization and nano-SiO₂ particles were synthesized by water-in-oil microemulsion approach, and metalloporphyrins were bonded to these nanoparticles by the medium of 3-aminopropyltriethoxysilane (APTES). The obtained nanoparticle bonded metalloporphyrins were characterized and their catalytic abilities were tested in the cyclohexane oxidation with PhIO. The relationship between the saturation magnetizations and catalytic abilities of these nanoparticle bonded metalloporphyrins was also discussed.

2 Experimental

2.1 Instruments and Reagents

The scanning electron microscopy (SEM) analyses were performed with a JSM-6700F Field Emission Scanning

C.-X. Liu · Q. Liu · C.-C. Guo (✉)
College of Chemistry and Chemical Engineering,
Hunan University, 410082 Changsha, China
e-mail: ccguo@hnu.cn

Electron Microscope. Magnetization measurements were performed at room temperature using Lake Shore 7410 vibration sample magnetometer (VSM). UV-visible spectra were recorded on a Shimadzu UV-240 spectrophotometer. IR spectra (KBr pellets) were recorded on a Thermo Nicolet NEXUS-670 Fourier transformation infrared spectrometer. The concentration of the iron ion in nanoparticles was determined with a Perkin–Elmer AA700 atomic absorption spectrophotometer (AAS). The oxidation products were confirmed by Shimadzu QP-2010 GC-MS and authentic samples, and were analyzed by a Shimadzu GC-2010 gas chromatograph (GC) equipped with a PEG-20 M column (25 m × 0.25 mm × 0.25 μm) and a flame ionization detector. The carrier gas was nitrogen. Injector and detector temperatures were both set at 200 °C and the oven temperature was set at 120 °C.

Three metalloporphyrin carboxylic acids, Manganese (III) 5-(*p*-carboxyphenyl)-10,15,20-triphenylporphyrin chloridize (MnCPTPPCl), Iron (III) 5-(*p*-carboxyphenyl)-10,15,20-triphenylporphyrin chloridize (FeCPTPPCl), Cobalt (II) 5-(*p*-carboxyphenyl)-10,15,20-triphenylporphyrin (CoCPTPP), were synthesized, purified and characterized according to the methodology in the literature [9]. Water used in all experimental procedures was deionized and doubly distilled prior to use. PhIO was synthesized following the method of Sharefkin and Saltzman [10, 11] by hydrolysis of iodophenylidacacetate, stored in a freezer and titrated before use. All the other reagents and solvents were obtained from commercial sources and used without further purification.

2.2 Preparation of Silica-coated Fe₃O₄ Nanoparticles with Different Saturation Magnetization

The magnetic Fe₃O₄ fluid was prepared by chemical coprecipitation. Ferrous chloride and ferric chloride with a mole ratio of 1:2 were added to water in a three-neck round bottom flask, and the solution was mechanically stirred. Then the ammonia was added into the solution. After stirring for 30 min, a magnet was held next to the flask, in dozens of seconds, the Fe₃O₄ nanoparticles were deposited on the wall of the reaction flask and the reaction mixture became transparent. Then, the reaction solution was decanted with the aid of a magnet. The Fe₃O₄ nanoparticles were redispersed in 10 mL water by sonicating for 5 min and recovered magnetically. After this process was repeated twice more, a series of magnetic Fe₃O₄ fluids **F(1)**, **F(2)**, **F(3)**, **F(4)**, **F(5)** were obtained by dispersing the Fe₃O₄ nanoparticles in different amount of water and the amount of Fe₃O₄ in these magnetic Fe₃O₄ fluids is 1.5 mg/mL, 3.1 mg/mL, 4.6 mg/mL, 6.2 mg/mL, 7.7 mg/mL, respectively.

Silica-coated Fe₃O₄ nanoparticles were synthesized by water-in-oil microemulsion approach. Cyclohexane (120 mL), 1-hexanol (30 mL) and Triton X-100 (30 mL)

were placed in a round bottom flask and the solution was mechanically stirred. Once the mixture was homogeneous system, the magnetic Fe₃O₄ fluid (5 mL) was placed into the flask. The suspension was continuous stirred 1 h, ammonium (4 mL) and tetraethyl orthosilicate (4 mL, TEOS) was then added in the flask. After the mixture was stirred at room temperature for 24 h, the reaction solution was easily decanted with the aid of the magnet. The obtained nanoparticles were redispersed in water (200 mL) by sonicating for 5 min, and separated magnetically. The nanoparticles were washed thoroughly with water and twice with ethanol as above. After third washing, the nanoparticles were dried under vacuum at 80 °C overnight and stored in a desiccator. When the different magnetic Fe₃O₄ fluids **F(1)**, **F(2)**, **F(3)**, **F(4)**, **F(5)** were used, corresponding silica-coated Fe₃O₄ nanoparticles **S(1)**, **S(2)**, **S(3)**, **S(4)**, **S(5)** were obtained.

2.3 Preparation of Nano-SiO₂ Particles

The nano-SiO₂ particles were prepared by the similar preparation procedure of silica-coated Fe₃O₄ nanoparticles. The difference is that an equal volume of water instead of the magnetic Fe₃O₄ fluid was added to the mixture of cyclohexane, 1-hexanol and Triton X-100. In addition, the obtained nano-SiO₂ particles were separated by centrifugation from the reaction solution. These nanoparticles were also washed thoroughly with water and twice with ethanol. After third washing, the nano-SiO₂ particles **S(0)** were dried under vacuum at 80 °C overnight and stored in a desiccator.

2.4 Preparation of Nanoparticle Bonded Metalloporphyrins

A solution of thionyl chloride (3 mL) and metalloporphyrin carboxylic acid (50 μmol) in chloroform (15 mL) were placed in a round bottom flask and the solution was refluxed for 3 h. Then, chloroform and excess thionyl chloride were distilled off under reduced pressure from the flask. After the obtained solid mixture was redissolved in 15 mL fresh chloroform, a solution of APTES (60 μmol) and triethylamine (0.25 mL) in chloroform (30 mL) was slowly added and the resultant reaction mixture was stirred for 1 h. After then, nanoparticles (340 mg, silica-coated Fe₃O₄ nanoparticles **S(1)**, **S(2)**, **S(3)**, **S(4)**, **S(5)** or nano-SiO₂ particles **S(0)**) were added and the volatiles were immediately evaporated via vacua. The obtained solid mixture was dried under vacuum at 110 °C. 3 h later, it was redispersed in 20 mL fresh chloroform by sonicating for 5 mixtures. The solid substance could be recovered by magnetic separation or centrifugation. This process was repeated twice more. After the third washing, the final products were dried under

vacuum overnight and stored in a desiccator. In this process, when the different metalloporphyrins, such as MnCPTPPCl, FeCPTPPCl, CoCPTPP, and nanoparticles **S(0)**, **S(1)**, **S(2)**, **S(3)**, **S(4)**, **S(5)** were used, corresponding nanoparticle bonded manganeseporphyrins **Mn(0)**, **Mn(1)**, **Mn(2)**, **Mn(3)**, **Mn(4)**, **Mn(5)**, nanoparticle bonded ironporphyrins **Fe(0)**, **Fe(1)**, **Fe(2)**, **Fe(3)**, **Fe(4)**, **Fe(5)**, and nanoparticle bonded cobaltporphyrins **Co(0)**, **Co(1)**, **Co(2)**, **Co(3)**, **Co(4)**, **Co(5)** could be obtained.

2.5 Measure of Saturation Magnetization

A certain amount of silica-coated Fe_3O_4 nanoparticles or silica-coated Fe_3O_4 nanoparticle bonded metalloporphyrins (ca. 10 mg) was accurately weighed and put into the sample tube. Its magnetic hysteresis loop was tested by VSM. The vertical axis and horizontal axis are magnetization (emu/g) and magnetic flux density (T), separately. A tangent was made from the point in the magnetic hysteresis loop corresponding to the maximum magnetic flux density. An intersection between the tangent and the vertical axis shall be the saturation magnetization of the sample.

2.6 Cyclohexane Oxidation with PhIO Catalyzed by Nanoparticle Bonded Metalloporphyrins

Under geomagnetic field (5×10^{-5} T), cyclohexane (10 mL) and nanoparticle bonded metalloporphyrins (94 mg, silica-coated Fe_3O_4 nanoparticle bonded metalloporphyrins or nano- SiO_2 particle bonded metalloporphyrins) were added to a 30 mL glass flask in inert atmosphere. The mixture was sonicated for 5 min at room temperature to disperse the solid substance. PhIO (100 mg) was then added and the reaction mixture was stirred at 30 °C. Upon completion of the reaction, the nanoparticle bonded metalloporphyrins were separated by magnetic separation or centrifugation. The reaction solutions were analyzed by GC and yields were figured by using chlorobenzene as internal standard.

2.7 Reuse of Nanoparticle Bonded Metalloporphyrins (**Fe(4)**, **Co(4)**, **Mn(4)**)

Upon completion of each reaction run, the reaction solution was magnetically decanted and analyzed by GC analysis. The isolated catalyst was washed with cyclohexane by the

procedure described in 2.2. Then, the recovered catalyst was dried under vacuum at room temperature. A new reaction run was started by the addition of a new batch of reagents and the mixture was sonicated for 5 min to redisperse the aggregated nanoparticle bonded metalloporphyrins into the solution. Recycling reactions were performed using the recovered catalyst as described above.

3 Results and Discussion

3.1 Preparation and Properties of Nanoparticles

Magnetic Fe_3O_4 nanoparticles could be easily prepared by chemical coprecipitation of ferrous chloride and ferric chloride. However, pure Fe_3O_4 nanoparticles are apt to hard-aggregates, and the magnetic properties would be changed because their structure could be changed in environment [12]. In order to overcome these drawbacks, silica coating is usually used to protect the magnetic Fe_3O_4 nanoparticles and carried out by water-in-oil microemulsion approach. This technique uses an oil-continuous microemulsion in which the water droplets can be regarded as nanoreactors [13]. Magnetic Fe_3O_4 nanoparticles would be equably dispersed in these nanoreactors after they were added. Silicon ester was then added and hydrolyzed in these nanoreactors. Upon completion of the reaction, silica-coated Fe_3O_4 nanoparticles with uniform nanoscale and sphericity could be obtained. In this process, the diameter of the obtained nanoparticles lies with the ratio of water and surface active agent in the microemulsion.

As shown in Scheme 1, the magnetic Fe_3O_4 fluids were added to the mixture of cyclohexane, 1-hexanol and Triton X-100, and the solution was stirred. After ammonium and TEOS were added and the solution was mechanically stirred for 24 h, silica-coated Fe_3O_4 nanoparticles **S(1)**, **S(2)**, **S(3)**, **S(4)**, **S(5)** were obtained. When the magnetic Fe_3O_4 fluid was replaced by water, the nano- SiO_2 particles **S(0)** could be obtained.

The contents of Fe_3O_4 in final products (**S(0)**, **S(1)**, **S(2)**, **S(3)**, **S(4)**, **S(5)**) can be measured by AAS and the results were shown in Table 1. We can see that the contents of Fe_3O_4 in nanoparticles increased with the increase of the Fe_3O_4 content in the added magnetic Fe_3O_4 fluid.

Scheme 1 Preparation of silica-coated Fe_3O_4 nanoparticles **S(1)**, **S(2)**, **S(3)**, **S(4)**, **S(5)**

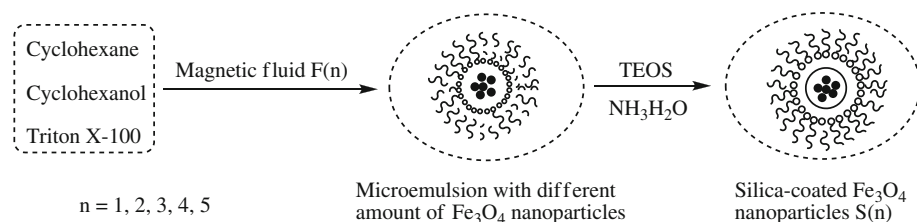


Table 1 Contents of Fe_3O_4 in nanoparticles

Nanoparticle	S(0)	S(1)	S(2)	S(3)	S(4)	S(5)
Content of Fe_3O_4 in magnetic fluid (mg/mL)	0	1.5	3.1	4.6	6.2	7.7
Content of Fe_3O_4 in nanoparticle (%)	0	13.7	22.7	29.3	38.3	54.3

The shape and scale of nanoparticles **S(0)**, **S(1)**, **S(2)**, **S(3)**, **S(4)**, **S(5)** were characterized by SEM (Fig. 1). The SEM images of **S(0)**, **S(1)**, **S(2)**, **S(3)**, **S(4)** show uniformity and spherical morphology, and their average diameter obtained by the particle size measurement results is ca. 58 nm. When the Fe_3O_4 content in magnetic Fe_3O_4 fluid equals 7.7 mg/mL, the scale and shape of the obtained silica-coated Fe_3O_4 nanoparticles **S(5)** are no longer uniform.

The magnetization curves of magnetic Fe_3O_4 nanoparticles and silica-coated Fe_3O_4 nanoparticles **S(1)**, **S(2)**, **S(3)**, **S(4)**, **S(5)** were shown in Fig. 2. The magnetization curves of all magnetic nanoparticles are similar. There is no hysteresis, and both remanence and coercivity are zero, suggesting that all magnetic nanoparticles are superparamagnetic. Moreover, with the increase of the Fe_3O_4 content, the saturation magnetizations of silica-coated Fe_3O_4 nanoparticles increased.

3.2 Synthesis and Characterization of Nanoparticle Bonded Metalloporphyrins

Though magnetic polymer microspheres immobilizing metalloporphyrins have been reported and the catalytic results in the cyclohexane oxidation with molecular oxygen have shown that these magnetic microspheres are highly efficient and recyclable catalysts [7, 8], the preparation of

the magnetic Fe_3O_4 nanoparticle bonded metalloporphyrins is still unprecedented. Due to the surface properties of magnetic iron oxide nanoparticles, especially chemically stable silica-coated Fe_3O_4 nanoparticles, organosilane is often used as a good medium to covalently bond organic compounds with magnetic nanoparticles. Therefore, most of magnetic nanocomposites with small molecular organic moieties reported were synthesized by the silanation reaction of silane-containing organic moieties with magnetic

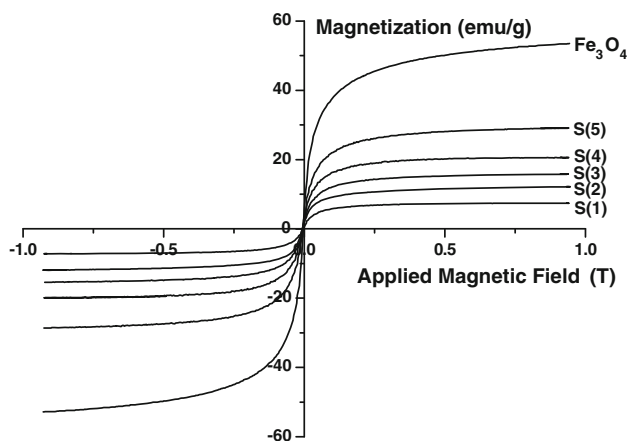


Fig. 2 Magnetization curves of magnetic Fe_3O_4 nanoparticles (Fe_3O_4) and silica-coated Fe_3O_4 nanoparticles **S(1)**, **S(2)**, **S(3)**, **S(4)**, **S(5)**

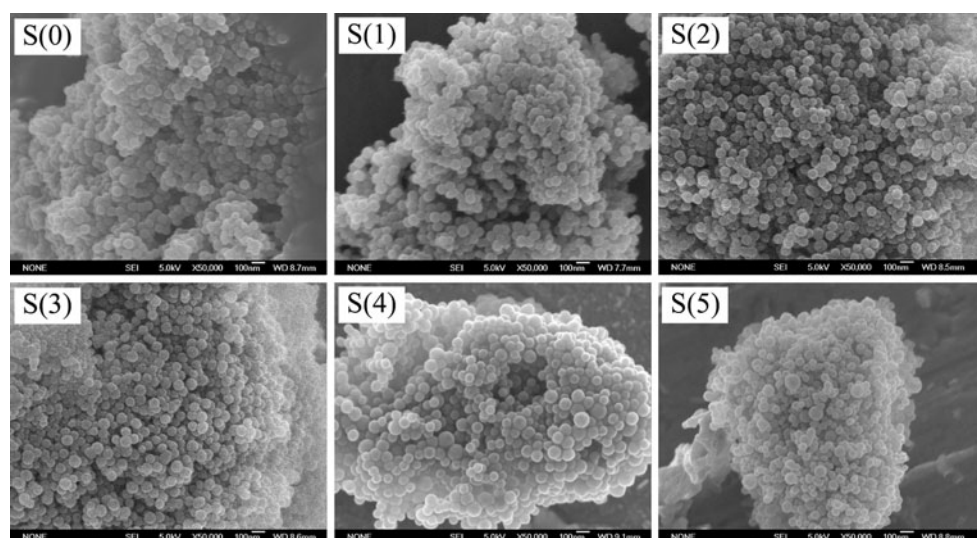


Fig. 1 SEM images of nano- SiO_2 particles **S(0)** and silica-coated Fe_3O_4 nanoparticles **S(1)**, **S(2)**, **S(3)**, **S(4)**, **S(5)**

iron oxide nanoparticles or silica-coated Fe_3O_4 nanoparticles in solution [14–18]. However, in this silanation method, the silane-containing organic moieties are prone to self-condensation [19], which is the main drawback of the effective immobilization of organic silane on magnetic nanoparticles.

To prepare silica-coated Fe_3O_4 nanoparticle bonded metalloporphyrins, metalloporphyrins acyl chloride should be first synthesized by the reaction of metalloporphyrins carboxylic acid (MnCPTPPCl , FeCPTPPCl , CoCPTPP) with SOCl_2 . Subsequent amidation of the acyl chloride with APTES afforded APTES derivatized metalloporphyrins (Scheme 2). And then, according to the standard silanation method mentioned above, APTES derivatized metalloporphyrins and silica-coated Fe_3O_4 nanoparticles should be refluxed in toluene to obtain silica-coated Fe_3O_4 nanoparticle bonded metalloporphyrins. However, much to our disappointment, the UV-vis analysis of the final solid products showed that no metalloporphyrin could be found, and this could not be improved by either adding more metalloporphyrin or using other solvents (e.g. hydrous toluene). The possible reasons are the self-condensation of

APTES derivatized metalloporphyrins and their poor solubility.

Fortunately, after the volatiles in the mixture of silica-coated Fe_3O_4 nanoparticles and the amidation reaction solution were evaporated via vacua, and the obtained solid mixture was processed under vacuum at 110 °C for 3 h (Scheme 2). The UV-vis analysis of the final product showed that metalloporphyrins were indeed present. When all metalloporphyrins (MnCPTPPCl , FeCPTPPCl , CoCPTPP) and nanoparticles **S(0)**, **S(1)**, **S(2)**, **S(3)**, **S(4)**, **S(5)** were used, the same things were happened. Thus, starting from metalloporphyrin carboxylic acids, corresponding nanoparticle bonded metalloporphyrins, such as nanoparticle bonded manganeseporphyrins **Mn(0)**, **Mn(1)**, **Mn(2)**, **Mn(3)**, **Mn(4)**, **Mn(5)**, nanoparticle bonded ironporphyrins **Fe(0)**, **Fe(1)**, **Fe(2)**, **Fe(3)**, **Fe(4)**, **Fe(5)**, and nanoparticle bonded cobaltporphyrins **Co(0)**, **Co(1)**, **Co(2)**, **Co(3)**, **Co(4)**, **Co(5)** could be easily obtained.

As shown in Fig. 3, the SEM images of silica-coated Fe_3O_4 nanoparticle bonded metalloporphyrins **Fe(4)**, **Co(4)**, **Mn(4)** show uniform diameter and spherical morphology, and they are similar to the SEM image of silica-

Scheme 2 Preparation of silica-coated Fe_3O_4 nanoparticle bonded metalloporphyrins

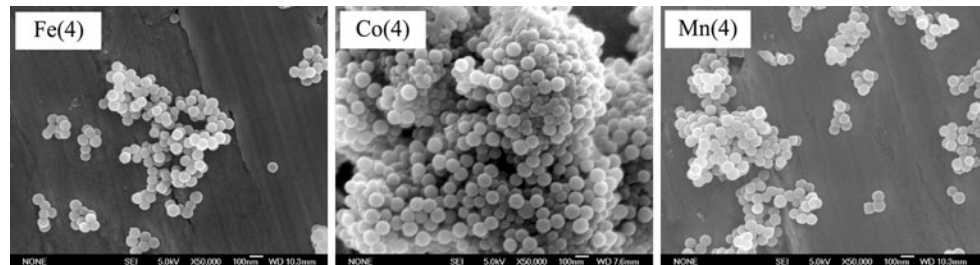
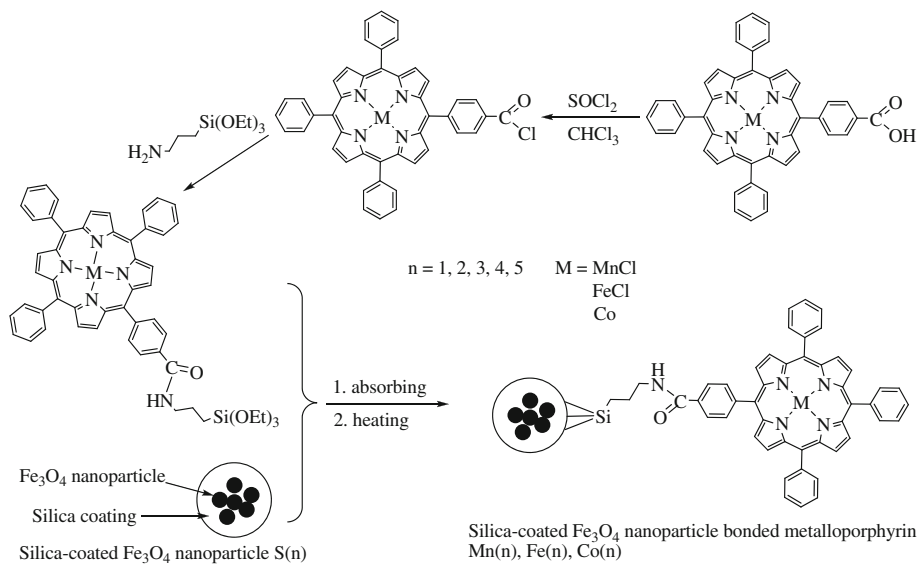


Fig. 3 SEM images of silica-coated Fe_3O_4 nanoparticle bonded metalloporphyrins **Fe(4)**, **Co(4)**, **Mn(4)**

coated Fe_3O_4 nanoparticles **S(4)**. These facts indicated retention of the silica-coated Fe_3O_4 nanoparticles structure during the silanation process.

The solid state UV-vis spectra of magnetic nanoparticle bonded metalloporphyrins (**Fe(4)**, **Co(4)**, **Mn(4)**) were measured and shown in Fig. 4. The Soret bands of manganeseporphyrin, ironporphyrin and cobaltporphyrin in the magnetic nanoparticle bonded metalloporphyrins **Fe(4)**, **Co(4)**, **Mn(4)** are at 482 nm, 413 nm, and 429 nm, respectively, and this is consistent with those of corresponding unsupported metalloporphyrins MnCPTPPCl , FeCPTPPCl , CoCPTPP , respectively. This fact indicated that the porphyrin macrocycles in the magnetic nanoparticle bonded metalloporphyrins remained intact after the silanation process.

To confirm the existence of Si–O–Si linkage between the metalloporphyrins and the nanoparticles, IR spectra in the wavenumbers of 4000–800 cm^{-1} of the silica-coated Fe_3O_4 nanoparticle bonded metalloporphyrins **Fe(4)**, **Co(4)**, **Mn(4)** and APTES were measured and displayed in Fig. 5. According to the literature, 1071 and 1040 cm^{-1} peaks assignable should be assigned to the Si–OEt and Si–O–Si groups, respectively [20]. Bands of 1750–1580 cm^{-1} should be fitted into three component peaks at 1675, 1657, and 1594 cm^{-1} , which are assigned to –CONH, –NH₂, and phenyl groups, respectively [21]. However, 1072 cm^{-1} peak assigned to the Si–OEt groups in APTES was translated into the peak at about 1040 cm^{-1} ascribed to Si–O–Si groups in the silica-coated Fe_3O_4 nanoparticle bonded metalloporphyrins **Fe(4)**, **Co(4)**, **Mn(4)**. These facts indicated that metalloporphyrins have been grafted to the outer surface of the nanoparticles successfully by Si–O–Si linkage.

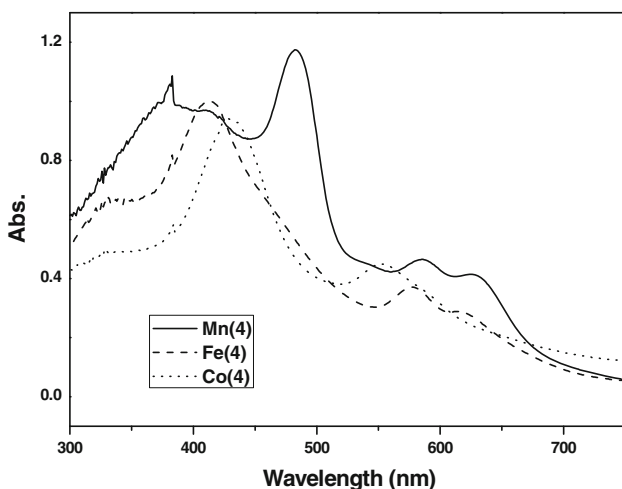


Fig. 4 Solid state UV-vis spectra of silica-coated Fe_3O_4 nanoparticle bonded metalloporphyrins **Fe(4)**, **Co(4)**, **Mn(4)**

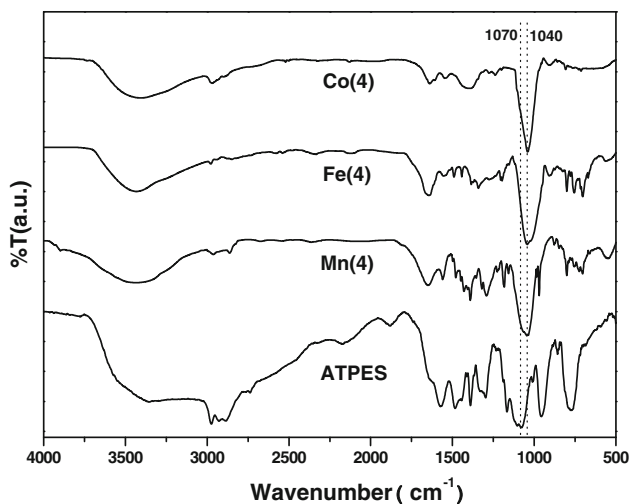


Fig. 5 IR spectra of silica-coated Fe_3O_4 nanoparticle bonded metalloporphyrins **Fe(4)**, **Co(4)**, **Mn(4)** and APTES

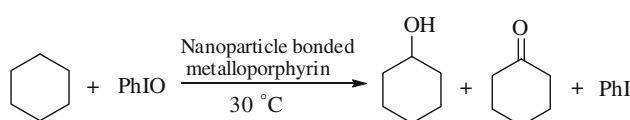
The magnetization curves of silica coated Fe_3O_4 nanoparticle bonded metalloporphyrins **Mn(1)**, **Mn(2)**, **Mn(3)**, **Mn(4)**, **Mn(5)**, **Fe(1)**, **Fe(2)**, **Fe(3)**, **Fe(4)**, **Fe(5)**, **Co(1)**, **Co(2)**, **Co(3)**, **Co(4)**, **Co(5)** were measured and compared with the ones of corresponding silica-coated Fe_3O_4 nanoparticles **S(1)**, **S(2)**, **S(3)**, **S(4)**, **S(5)**. These curves showed that all silica coated Fe_3O_4 nanoparticle bonded metalloporphyrins still maintained superparamagnetic. As shown in Table 2, the saturation magnetizations of all silica coated Fe_3O_4 nanoparticle bonded metalloporphyrins were lower than the ones of corresponding silica-coated Fe_3O_4 nanoparticles, and unrelated to the type of metalloporphyrins. It indicated that the magnetizations of all silica coated Fe_3O_4 nanoparticle bonded metalloporphyrins come from the corresponding silica-coated Fe_3O_4 nanoparticles.

3.3 Influence of the Saturation Magnetizations on the Catalytic Abilities of Nanoparticle Supported Metalloporphyrins in the Cyclohexane Oxidation

In order to study the influence of the saturation magnetizations on the catalytic abilities of nanoparticle bonded metalloporphyrins under geomagnetic field ($5 \times 10^{-5} \text{ T}$),

Table 2 Saturation magnetizations of silica-coated Fe_3O_4 nanoparticle bonded metalloporphyrins

n	S(n)	Fe(n)	Mn(n)	Co(n)
1	7.3	6.29	6.27	6.32
2	12.1	10.53	10.49	10.56
3	15.6	13.71	13.68	13.73
4	20.4	17.86	17.82	17.89
5	28.9	24.95	24.92	24.97



Scheme 3 Oxidation of cyclohexane with PhIO catalyzed by nanoparticle bonded metalloporphyrins

the catalytic abilities of all nanoparticle bonded metalloporphyrins with different saturation magnetization were investigated through the cyclohexane oxidation with PhIO to produce cyclohexanol and cyclohexanone (Scheme 3).

The yields of cyclohexanol in the cyclohexane oxidation catalyzed by nanoparticle bonded metalloporphyrins with different saturation magnetization were shown in Table 3. Control test using silica-coated Fe_3O_4 nanoparticles as catalysts gave no cyclohexanol and cyclohexanone at all even after 12 h (data not shown). This showed that metalloporphyrin catalyst was necessary for the cyclohexane oxidation with PhIO. As shown in Table 3, we noted that (i) under the same case, the yields of cyclohexanol in the cyclohexane oxidation catalyzed by nanoparticle bonded cobaltporphyrins are lower than the ones catalyzed by corresponding nanoparticle bonded manganeseporphyrins

or nanoparticle bonded ironporphyrins; (ii) with the increase of the saturation magnetizations, the yields of cyclohexanol in the cyclohexane oxidation catalyzed by nanoparticle bonded manganeseporphyrins or nanoparticle bonded ironporphyrins obviously increased, but the growth of the ones catalyzed by nanoparticle bonded cobaltporphyrins was not obvious; (iii) compared with the yields of cyclohexanol in the cyclohexane oxidation catalyzed by non-magnetic nanoparticle bonded metalloporphyrins (**Fe(0)**, **Co(0)**, **Mn(0)**), the growth rate of the ones catalyzed by magnetic nanoparticle bonded metalloporphyrins (**Fe(5)**, **Co(5)**, **Mn(5)**) followed the order of ironporphyrin > manganeseporphyrin > cobaltporphyrin. This is consistent with the results obtained by metalloporphyrins under the external magnetic field [6], and indicates that it is natural choice for cytochrome P-450 mono-oxygenase with ironporphyrin structure. Therefore, it will be significant to reveal the mysteries of biology and the Earth.

These experimental results could be explained by the spin state of the central metal ion in metalloporphyrins. When the central metal ion is high-spin state, the catalytic abilities of metalloporphyrins are better [22, 23]. The spin state of the central metal ion is controlled by the axial

Table 3 Yields of cyclohexanol in the cyclohexane oxidation catalyzed by nanoparticle bonded metalloporphyrins with different saturation magnetization^a

Metalloporphyrin	Nanoparticle bonded metalloporphyrins	Saturation Magnetization ^b (emu/g)	Yields of Cyclohexanol (%)
Ironporphyrin	Fe(0)	0	15.8
	Fe(1)	6.29	17.3
	Fe(2)	10.53	18.5
	Fe(3)	13.71	19.3
	Fe(4)	17.86	20.2
	Fe(5)	24.95	20.9
Manganeseporphyrin	Mn(0)	0	15.6
	Mn(1)	6.27	17.1
	Mn(2)	10.49	17.9
	Mn(3)	13.68	18.7
	Mn(4)	17.82	19.1
	Mn(5)	24.92	19.8
Cobaltporphyrin	Co(0)	0	6.4
	Co(1)	6.32	6.5
	Co(2)	10.56	6.6
	Co(3)	13.73	6.7
	Co(4)	17.89	6.8
	Co(5)	24.97	6.8

^a Reaction conditions: 94 mg nanoparticle bonded metalloporphyrins (13.4 μmol metalloporphyrins), 100 mg PhIO in 10 mL cyclohexane at 30 °C in inert atmosphere. The average magnetic field intensity of the geomagnetic field is ca. 5×10^{-5} T. The products were detected by GC using chlorobenzene as internal standard. The yields (%) are based on PhIO and were obtained when the amount of cyclohexanol showed no further increase in the reaction solution

^b Saturation magnetizations of nanoparticle bonded metalloporphyrins

Table 4 Yields of cyclohexanol and cyclohexanone in the cyclohexane oxidation catalyzed by silica-coated Fe_3O_4 nanoparticle bonded metalloporphyrins **Fe(4)**, **Co(4)**, **Mn(4)^a**

Catalyst	Yield (%)					
	1st run C-ol/Total	2nd run C-ol/Total	3rd run C-ol/Total	4th run C-ol/Total	5th run C-ol/Total	6th run C-ol/Total
Mn(4)	19.1/32.1	18.7/31.4	18.3/30.5	17.3/29.5	16.8/28.6	15.2/26.8
Fe(4)	20.2/32.5	19.4/31.8	19.1/30.7	18.3/29.8	17.5/28.4	15.6/26.1
Co(4)	6.8/12.2	6.7/11.5	6.4/10.9	5.5/9.8	4.8/8.7	3.6/6.8

^a Conditions see Table 3

ligands of metalloporphyrins [24]. When the axial ligands of manganeseporphyrin or ironporphyrin studied are chlorides, which are moderate field ligands, they are in high spin state [24, 25]. However, the cobalt ion in cobaltporphyrin is in low spin state. As a result, the single-electron numbers of the central metal ion in ironporphyrin, manganeseporphyrin and cobaltporphyrin are 5, 4 and 1, respectively. So the influence of the saturation magnetizations on the catalytic abilities of three metalloporphyrins followed the order of ironporphyrin > manganeseporphyrin > cobaltporphyrin.

3.4 Reuse of Nanoparticle Bonded Metalloporphyrins (**Fe(4)**, **Co(4)**, **Mn(4)**)

From Table 4, we can see that three nanoparticle bonded metalloporphyrins (**Fe(4)**, **Co(4)**, **Mn(4)**) could be recovered and reused for 5 times, only showing minor loss of activity during the last runs. This fact indicated that the silica-coated Fe_3O_4 nanoparticles are really good carriers and the combination between metalloporphyrins silica-coated Fe_3O_4 nanoparticles is really strong.

4 Conclusions

In summary, a series of silica-coated Fe_3O_4 nanoparticle bonded metalloporphyrins with different saturation magnetization and nano- SiO_2 particle bonded metalloporphyrins were successfully synthesized and their catalytic abilities were tested in the cyclohexane oxidation with PhIO. Under geomagnetic field (5×10^{-5} T), a positive relationship really exist between the saturation magnetizations of these nanoparticle bonded metalloporphyrins and the catalytic abilities of metalloporphyrins. The growth rate of yields of cyclohexanol in the cyclohexane oxidation catalyzed by three metalloporphyrins follows the order of ironporphyrin > manganeseporphyrin > cobaltporphyrin.

Acknowledgement The authors gratefully thank the financial supports of National Natural Science Foundation of China (Grants CN J0830415).

References

- Blakemore R (1975) *Science* 190:377
- Herve P, Nome F, Fendler JH (1984) *J Am Chem Soc* 106:8291
- Mansuy D (2007) *C R Chim* 10:392
- Nam W, Park SE, Lim IK, Lim MH, Hong J, Kim J (2003) *J Am Chem Soc* 125:14674
- Doyle MP (2009) *Angew Chem Int Ed* 48:850
- Guo CC, Hao XD, Zhang XB, Liang BX, Chen XB (1997) *Chem J Chinese U* 18:906 (in Chinese)
- Fu B, Yu HC, Huang JW, Zhao P, Liu J, Ji LN (2009) *J Mol Catal A* 298:74
- Fu B, Zhao P, Yu HC, Huang JW, Liu J, Ji LN (2009) *Catal Lett* 127:411
- Hansen CB, Hoogers GJ, Drenth W (1993) *J Mol Catal* 79:153
- Sharefkin JG, Saltzmann H (1963) *Org Synth* 43:62
- Lucas HJ, Kennedy ER, Forno MW (1963) *Org Synth* 43:483
- Lu AH, Salabas EL, Schüth F (2007) *Angew Chem Int Ed* 46:1222
- Santra S, Tapec R, Theodoropoulou N, Dobson J, Hebard A, Tan W (2001) *Langmuir* 17:2900
- Dálaigh CÓ, Corr SA, Gun'ko Y, Connolly SJ (2007) *Angew Chem Int Ed* 46:4329
- Gill CS, Price BA, Jones CW (2007) *J Catal* 251:145
- Luo SZ, Zheng XX, Cheng JP (2008) *Chem Commun* 5719
- Xie WL, Ma N (2009) *Energy Fuels* 23:1347
- Jiang YY, Guo C, Xia HS, Mahmood I, Liu CZ, Liu HZ (2009) *J Mol Catal B* 58:103
- Wu PG, Xu ZH (2005) *Ind Eng Chem Res* 44:816
- Kishida T, Fujita N, Sada K, Shinkai S (2005) *J Am Chem Soc* 127:7298
- Imahori H, Mitamura K, Shibano Y, Umeyama T, Matano Y, Yoshida K, Isoda S, Araki Y, Ito O (2006) *J Phys Chem B* 110:11399
- Hill CL (1989) Activation and functionalization of alkanes. Interscience Publication, Wiley
- Guo CC, Li ZP, Liang BX, Zhang XB (1996) *J Hunan U* 23:66 (in Chinese)
- Scheidt WR, Reed CA (1981) *Chem Rev* 81:543 and references therein
- Lü QZ, Yu RQ, Shen GL (2003) *J Mol Catal A* 198:9